

# INDC International Nuclear Data Committee

## Results of Time-of-Flight Transmission Measurements for $^{103}\text{Rh}$ at a 10 m Station of GELINA

Y. K. Kim<sup>a</sup>, V. Chavan<sup>a</sup>, C. Paradela<sup>b</sup>, G. Alaerts<sup>b</sup>, S. I. Bak<sup>a</sup>, J. Heyse<sup>b</sup>, S. Kopecky<sup>b</sup>,  
A. Oprea<sup>c</sup>, P. Schillebeeckx<sup>b</sup>, R. Wynants<sup>b</sup> and S. W. Hong<sup>a</sup>

<sup>a</sup> Department of Physics, Sungkyunkwan University, Suwon, Republic of Korea

<sup>b</sup> European Commission Joint Research Centre, Geel, Belgium

<sup>c</sup> Horia Hulubei National Institute of Physics and Nuclear Engineering, Magurele, Romania

March 2019

Selected INDC documents may be downloaded in electronic form from

<http://www-nds.iaea.org/publications/>

or sent as an e-mail attachment.

Requests for hardcopy or e-mail transmittal should be directed to

[nds.contact-point@iaea.org](mailto:nds.contact-point@iaea.org)

or to:

Nuclear Data Section  
International Atomic Energy Agency  
Vienna International Centre  
PO Box 100  
A-1400 Vienna  
Austria

Produced by the IAEA in Austria  
March 2019

## Results of Time-of-Flight Transmission Measurements for $^{103}\text{Rh}$ at a 10 m Station of GELINA

Y. K. Kim<sup>a</sup>, V. Chavan<sup>a</sup>, C. Paradela<sup>b</sup>, G. Alaerts<sup>b</sup>, S. I. Bak<sup>a</sup>, J. Heyse<sup>b</sup>, S. Kopecky<sup>b</sup>,  
A. Oprea<sup>c</sup>, P. Schillebeeckx<sup>b</sup>, R. Wynants<sup>b</sup> and S. W. Hong<sup>a</sup>

<sup>a</sup> Department of Physics, Sungkyunkwan University, Suwon, Republic of Korea

<sup>b</sup> European Commission Joint Research Centre, Geel, Belgium

<sup>c</sup> Horia Hulubei National Institute of Physics and Nuclear Engineering, Magurele, Romania



March 2019



# Results of time-of-flight transmission measurements for $^{103}\text{Rh}$ at a 10 m station of GELINA

*Y. K. Kim<sup>a</sup>, V. Chavan<sup>a</sup>, C. Paradela<sup>b</sup>, G. Alaerts<sup>b</sup>, S. I. Bak<sup>a</sup>, J. Heyse<sup>b</sup>, S. Kopecky<sup>b</sup>, A. Oprea<sup>c</sup>,  
P. Schillebeeckx<sup>b</sup>, R. Wynants<sup>b</sup> and S. W. Hong<sup>a</sup>*

<sup>a</sup>Department of Physics, Sungkyunkwan University, Suwon 16419, Republic of Korea

<sup>b</sup>European Commission, Joint Research Centre, B - 2440 Geel, Belgium

<sup>c</sup>Horia Hulubei National Institute of Physics and Nuclear Engineering, Magurele, Romania

**Abstract.** Transmission measurements have been performed at the time-of-flight facility GELINA to determine neutron resonance parameters for  $^{103}\text{Rh}$ . The measurements have been carried out at a 10 m transmission station at a moderated neutron beam using a Li-glass scintillator with the accelerator operating at 800 Hz and 50 Hz. This report provides the experimental details required to deliver the data to the EXFOR data library which is maintained by the Nuclear Data Section of the IAEA and the Nuclear Energy Agency of the OECD. The experimental conditions and data reduction procedures are described. In addition, the full covariance information based on the AGS concept is given such that nuclear reaction model parameters together with their covariances can be derived in a least squares adjustment to the data.

## 1 Introduction

To study the resonance structure of neutron induced reaction cross sections, neutron spectroscopic measurements are required which determine with a high accuracy the energy of the neutron that interacts with the material under investigation. To cover a broad energy range such measurements are best carried out with a pulsed white neutron source, which is optimized for time-of-flight (TOF) measurements [1].

The TOF-facility GELINA [2][3] has been designed and built for high-resolution cross section measurements in the resonance region. It is a multi-user facility, providing a white neutron source with a neutron energy range from 10 meV to 20 MeV. Up to 10 experiments can be performed simultaneously at measurement stations located between 10 m to 400 m from the neutron production target. The electron linear accelerator

provides a pulsed electron beam with a maximum energy of 150 MeV, a peak current of 10 A and a repetition rate ranging from 50 Hz to 800 Hz. A compression magnet reduces the width of the electron pulses to about 2 ns [4]. The electron beam hits a mercury-cooled uranium target producing Bremsstrahlung and subsequently neutrons via photonuclear reactions [5]. Two water-filled beryllium containers mounted above and below the neutron production target are used to moderate the neutrons. By applying different neutron beam collimation conditions, experiments can use either a fast or a moderated neutron spectrum. The neutron production rate is monitored by  $\text{BF}_3$  proportional counters which are mounted in the ceiling of the target hall. The output of the monitors is used to normalize the time-of-flight spectra to the same neutron intensity. The measurement stations are equipped with air conditioning to reduce electronic drifts in the detection chains due to temperature changes.

In this report results of transmission measurements carried out at GELINA with  $^{103}\text{Rh}$  metallic samples are described. To reduce bias effects due to e.g. dead time and background, the measurement and data reduction procedures recommended in Ref. [1], have been followed. The main objective of this report is to provide the information that is required to extract resonance parameters for  $^{103}\text{Rh}$  in a least squares adjustment to the data using e.g. the resonance shape analysis code REFIT [6]. In the description of the data the recommendations resulting from a consultant's meeting organized by the Nuclear Data Section of the IAEA have been followed [7].

## 2 Experimental conditions

The transmission experiments were performed at the 10 m measurement station of flight path 13 with the accelerator operating at 800 Hz and 50 Hz. The moderated neutron spectrum was used. A shadow bar made of Cu and Pb was placed close to the uranium target to reduce the intensity of the  $\gamma$ -ray flash and the fast neutron component. The flight path forms an angle of  $18^\circ$  with the direction normal to the face of the moderator viewing the flight path. The samples and detector were placed in a acclimatized room to keep them at a constant temperature of  $20^\circ\text{C}$ .

The partially thermalized neutrons scattered from the moderators were collimated into the flight path through an evacuated aluminium pipe of 50 cm diameter with annular collimators, consisting of borated wax, copper and lead. A set of Pb, Ni and Cu annular collimators was used to reduce the neutron beam to a diameter of 10 mm at the sample position. Additional lithium and B<sub>4</sub>C collimators were installed to absorb neutrons that are scattered by the collimators [8]. The samples were placed at 7.7 m distance from the neutron source. Close to the sample position a 4 mm Cd overlap filter was placed to absorb slow neutrons from a previous burst. When the accelerator is operated at 50 Hz the measurement is performed without the overlap filter. The impact of the  $\gamma$ -ray flash was reduced by a Pb filter. Permanent Na, Co, W and Ag black resonance filters were used to continuously monitor the background at 2850 keV, 132 eV, 21.1 eV and 5.2 eV and to account for the impact of the sample on the background [1]. The neutron beam passing through the sample and filters was further collimated and detected by a 6.35 mm x 76 mm x 76 mm Scionix Li-glass scintillator. The detector was placed at about 11 m from the neutron target.

The TOF of the detected neutron was derived from the time difference between the stop signal  $T_s$ , obtained from the anode impulse of the PMT, and the start signal  $T_0$ , given at each electron burst. This time difference was processed with a multi-hit fast time coder with a 0.5 ns time resolution [9]. The TOF and the pulse height of each detected event were recorded in list mode using a multi-parameter data acquisition system developed at the EC-JRC [10]. Each measurement was subdivided in different cycles. Only cycles for which the ratio between the total counts in the transmission detector and in the neutron monitor deviated by less than 1 % were selected. The dead time of the detection chain  $t_d = (3024 \pm 10)$  ns was derived from a spectrum of the time-interval between successive

events. The uncertainties due to dead time corrections in the region of interest are very small and can be neglected.

All measurements were performed with  $^{103}\text{Rh}$  metallic samples. The main characteristics of the samples are reported in Table 1. For the 0.75 mm of Rh sample, a stack of three samples of thicknesses 0.3, 0.3 and 0.15 mm each were used. The areal density of the natural samples was derived from a measurement of the weight and the area with an uncertainty better than 0.1 %. The mass was determined by substitution weighing with a microbalance from Mettler Toledo. The area was determined by an optical surface inspection with a microscope system from Mitutoyo [11].

ID	Thickness /mm	Mass/g	Area/mm <sup>2</sup>	Areal Density (at/b)
1	0.075	0.58894 (2)	626.20 (2)	5.4987 (2) $\times 10^{-4}$
2	0.15	4.63518 (3)	2505.3 (8)	1.0818 (3) $\times 10^{-3}$
3.1	0.3	8.98856 (6)	2467.8 (5)	2.1295 (4) $\times 10^{-3}$
3.2	0.3	9.24940 (7)	2494.69 (6)	2.16771 (5) $\times 10^{-3}$
3.3	0.15	4.56431 (3)	2472.28 (14)	1.07940 (6) $\times 10^{-3}$

Table 1 Characteristics of the samples used for the transmission measurements. Each areal density  $n_d$  was calculated by using the experimentally determined mass and area.

### 3 Data reduction

The AGS code [12][13], developed at the EC-JRC, was used to derive the experimental transmission from the TOF-spectra. The code is based on a compact formalism to propagate all uncertainties starting from uncorrelated uncertainties due to counting statistics.

#### 3.1 Experimental transmission

The experimental transmission  $T_{\text{exp}}$  as a function of TOF was obtained from the ratio of a sample-in measurement  $C_{\text{in}}$  and a sample-out measurement  $C_{\text{out}}$ , both corrected for their background contributions  $B_{\text{in}}$  and  $B_{\text{out}}$ , respectively:

$$T_{\text{exp}} = N \frac{C_{\text{in}} - KB_{\text{in}}}{C_{\text{out}} - KB_{\text{out}}}, \quad (3.1)$$

The TOF spectra ( $C_{\text{in}}$ ,  $C_{\text{out}}$ ,  $B_{\text{in}}$ ,  $B_{\text{out}}$ ) were corrected for losses due to the dead time in the detector and electronics chain. All spectra were normalized to the same TOF-bin width structure and neutron beam intensity. The latter was derived from the response of the  $\text{BF}_3$  beam monitors. To avoid systematic effects due to slow variations of both the beam intensity and detector efficiency as a function of time, data were taken by alternating sample-in and sample-out measurements in cycles of about 600 seconds. Such a procedure reduces the uncertainty on the normalization to the beam intensity to less than 0.25 %. This uncertainty was evaluated from the ratios of counts in the  $^6\text{Li}$  transmission detector and in the flux monitors. To account for this uncertainty the factor  $N = 1.0000$  (25) was introduced in Eq. (3.1). The background as a function of TOF was approximated by an analytic expression applying the black resonance technique [1]. The factor  $K = 1.00$  (3) in Eq. (3.1) was introduced to account for systematic effects due to the background model. Its uncertainty was derived from a statistical analysis of the difference between the observed black resonance dips and the estimated background [16]. This uncertainty is only valid for measurements with at least two fixed black resonance filters in the beam [1].

The time-of-flight ( $t$ ) of a neutron creating a signal in the neutron detector was determined by the time difference between the start signal ( $T_0$ ) and the stop signal ( $T_s$ ):

$$t = (T_s - T_0) + t_0, \quad (3.2)$$

with  $t_0$  a time-offset which was determined by a measurement of the  $\gamma$ -ray flash. The flight path distance  $L = 10.860$  (1) m, i.e. the distance between the centre of the moderator viewing the flight path and the front face of the detector, was derived previously from results of transmission measurements using uranium standard references.

### 3.2 Background correction

The background as a function of TOF was parametrized by an analytical expression consisting of a constant and two exponentials:

$$B(t) = b_0 + b_1 e^{-\lambda_1 t} + b_2 e^{-\lambda_2 t} + b_3 e^{-\lambda_3(t+t_0)} \quad (3.3)$$

The parameter  $b_0$  is the time independent contribution. The first exponential is due to the detection of 2.2 MeV  $\gamma$ -rays resulting from neutron capture in hydrogen present in the moderator. The second exponential originates predominantly from neutrons scattered inside the detector station. The third one is due to slow neutrons from previous accelerator cycles. This contribution was estimated by an extrapolation of the TOF-spectrum at the end of the cycle. The time shift  $\tau_0$  is the inverse of the accelerator frequency, i.e.  $\tau_0 = 1.25$  ms for 800 Hz and 20 ms for 50 Hz. The time dependence of the background was derived from the results of measurements with the 0.15 mm thick Rh sample and verified with measurements using a 3 mm thick Au sample. The dead time corrected sample-in TOF-spectrum together with the background contributions resulting from the measurements with the 0.15 mm thick  $^{103}\text{Rh}$  sample and Na, Co, W and Ag black resonance filters is shown in Figure 1, whereas Figure 2 shows the spectrum corresponding to the 0.75 mm thick  $^{103}\text{Rh}$  sample and Na, Co, W and Ag filters.

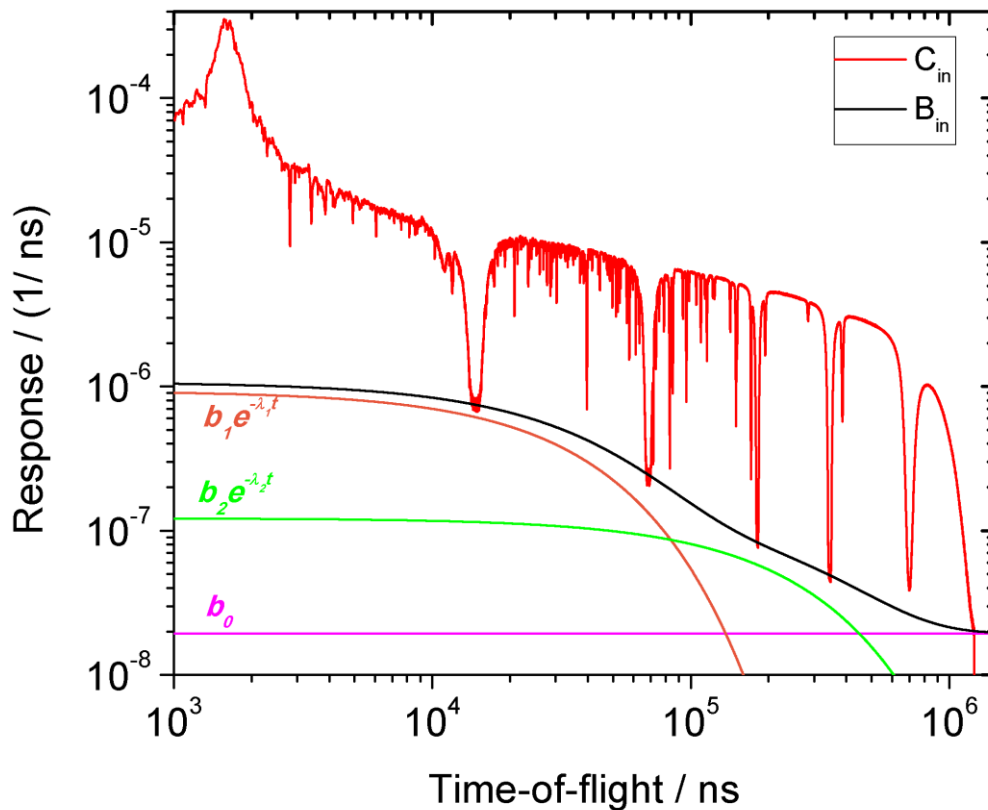


Figure 1. TOF spectrum with the 0.15 mm thick  $^{103}\text{Rh}$  sample ( $C_{in}$ ) in the beam at 800 Hz together with the total background ( $B_{in}$ ) and its different components.



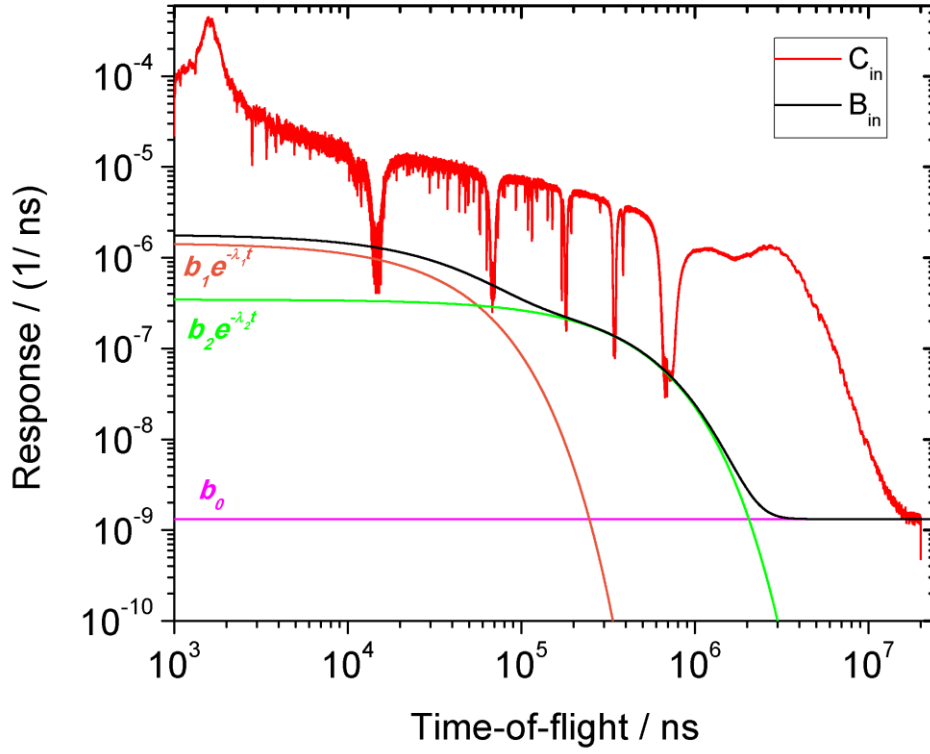


Figure 2. TOF spectrum with the 0.75 mm thick  $^{103}\text{Rh}$  sample ( $C_{\text{in}}$ ) in the beam at 50Hz together with the total background ( $B_{\text{in}}$ ) and its different components.

ID	$b_0/10^{-8}$ $\text{ns}^{-1}$	$b_1/10^{-7}$ $\text{ns}^{-1}$	$\lambda_1/10^{-5}$ $\text{ns}^{-1}$	$b_2/10^{-7}$ $\text{ns}^{-1}$	$\lambda_2/10^{-6}$ $\text{ns}^{-1}$
$B_{\text{in}}$	2.04	9.17	-2.84	1.26	-4.34
$B_{\text{out}}$	2.08	9.25	-2.84	1.24	-4.26

Table 2. Parameters for the analytical expressions of the background correction for the sample-in and sample-out measurements for the rhodium sample of 0.075 mm measured at the 800 Hz linac frequency. Parameter uncertainties are smaller than reported digits.

ID	$b_0/10^{-8}$ $\text{ns}^{-1}$	$b_1/10^{-7}$ $\text{ns}^{-1}$	$\lambda_1/10^{-5}$ $\text{ns}^{-1}$	$b_2/10^{-7}$ $\text{ns}^{-1}$	$\lambda_2/10^{-6}$ $\text{ns}^{-1}$
$B_{\text{in}}$	1.94	9.30	-2.84	1.22	-4.11
$B_{\text{out}}$	2.09	9.31	-2.84	1.24	-4.25

Table 3. Parameters for the analytical expressions of the background correction for the sample-in and sample-out measurements for the rhodium sample of 0.15 mm measured at the 800 Hz linac frequency. Parameter uncertainties are smaller than reported digits.

ID	$b_0/10^{-9}$ $\text{ns}^{-1}$	$b_1/10^{-6}$ $\text{ns}^{-1}$	$\lambda_1/10^{-5}$ $\text{ns}^{-1}$	$b_2/10^{-7}$ $\text{ns}^{-1}$	$\lambda_2/10^{-6}$ $\text{ns}^{-1}$
$B_{\text{in}}$	1.38	1.44	-2.5	3.19	-2.6
$B_{\text{out}}$	1.39	1.49	-2.5	3.15	-2.6

Table 4. Parameters for the analytical expressions of the background correction for the sample-in and sample-out measurements for the rhodium sample of 0.75 mm measured at 50 Hz linac frequency. Parameter uncertainties are smaller than reported digits.

## 4 Results

The AGS code [12][13] was used to derive the experimental transmission and propagate both the correlated and uncorrelated uncertainties. The code is based on a compact formalism to propagate all uncertainties starting from uncorrelated uncertainties due to counting statistics. It stores the full covariance information after each operation in a concise, vectorized way. The AGS formalism results in a substantial reduction of data storage volume and provides a convenient structure to verify the various sources of uncertainties through each step of the data reduction process. The concept is recommended by the NDS/IAEA [7] to prepare the experimental observables, including their full covariance information, for storage into the EXFOR data library [14].

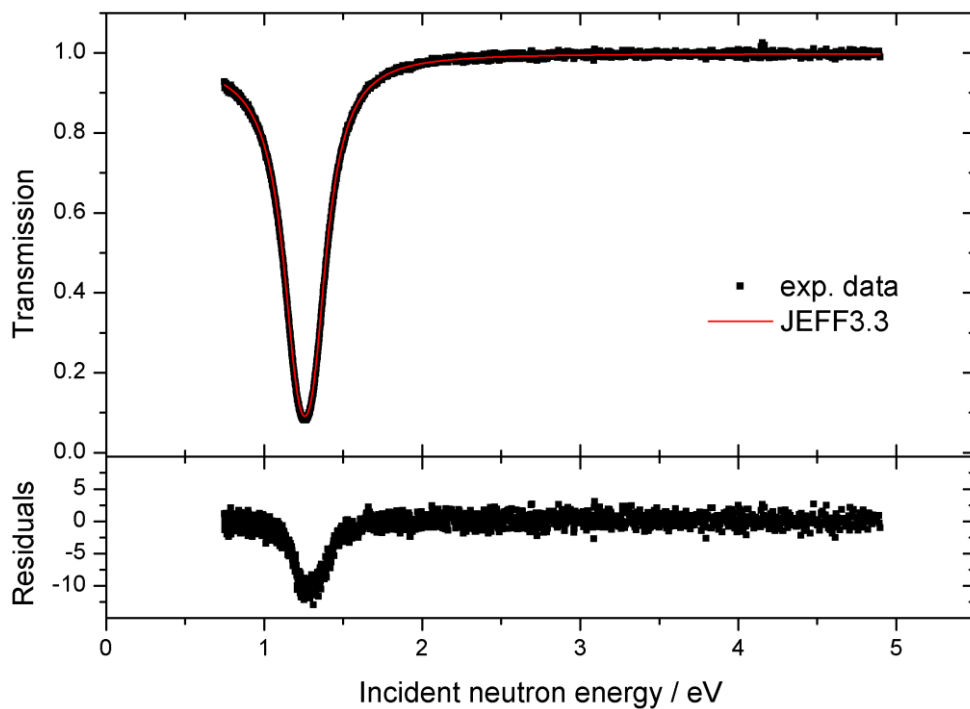


Figure 3. Experimental transmission as a function of time-of-flight resulting from measurements with the 0.075 mm thick  $^{103}\text{Rh}$  sample at 800 Hz in the energy region 0.5-5 eV compared with the transmission spectrum calculated with REFIT by using resonance parameters provided in JEFF-3.3 evaluation.

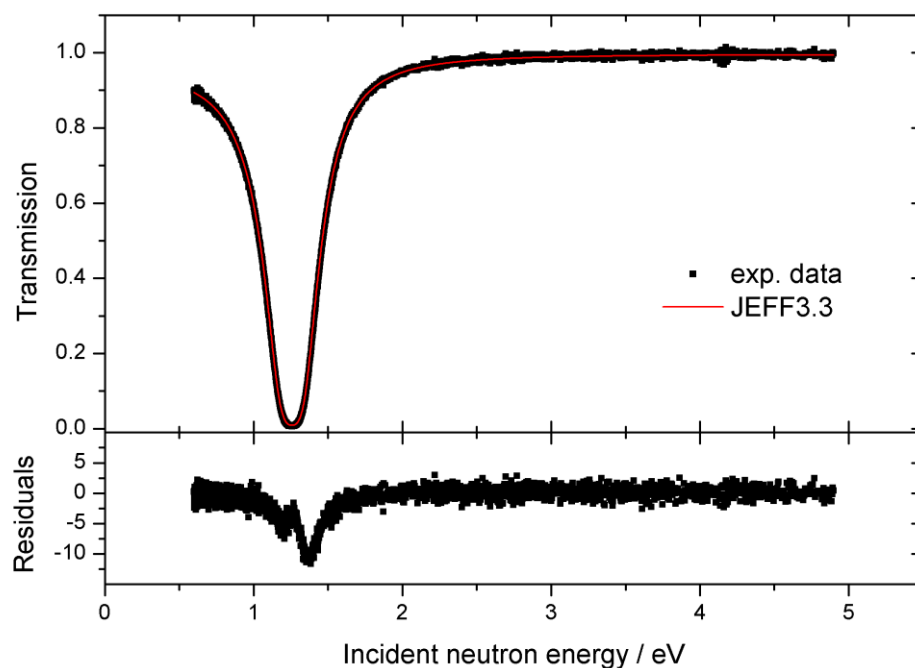


Figure 4. Experimental transmission as a function of time-of-flight resulting from measurements with the 0.15 mm thick  $^{103}\text{Rh}$  sample at 800 Hz in the energy region 0.5-5 eV compared with the transmission spectrum calculated with REFIT and JEFF-3.3 evaluation.

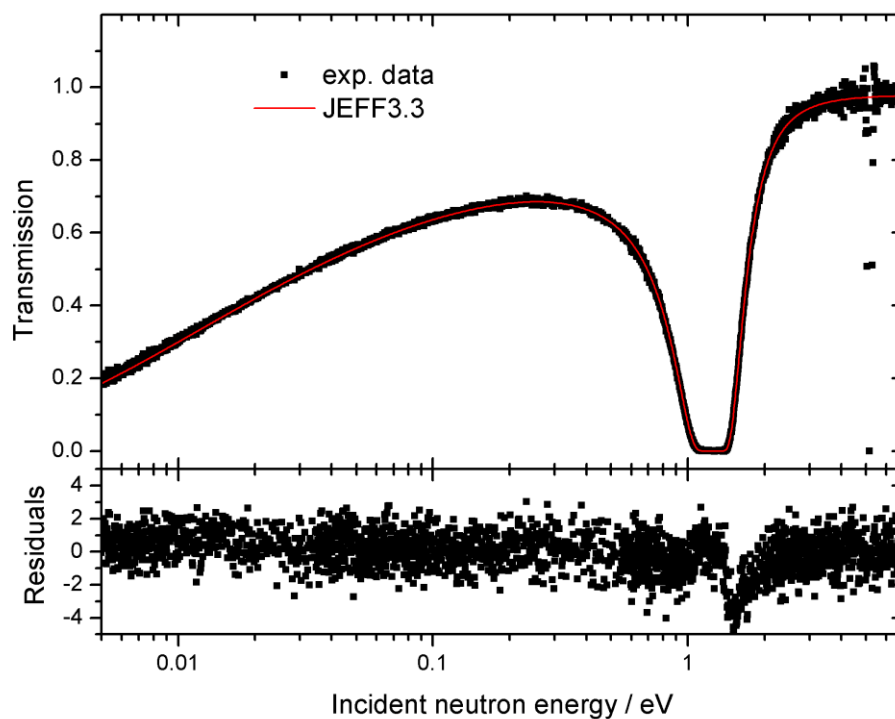


Figure 5. Experimental transmission as a function of time-of-flight resulting from measurements with the 0.75 mm thick  $^{103}\text{Rh}$  sample at 50 Hz in the energy region 0.01-5 eV compared with the transmission spectrum calculated with REFIT and JEFF-3.3 evaluation.

The experimental transmissions resulting from the measurements with three different samples are shown in Figure 3, 4 and 5. In the case of the 0.075 mm thick sample, the experimental transmission is compared with the transmission calculated with the resonance parameters in the JEFF-3.3 evaluation library. The format in which the numerical data will be stored in the EXFOR data library is illustrated in the Appendix. The data include the full covariance information based on the AGS concept. The total uncertainty and the uncertainty due to uncorrelated components are reported, together with the contributions due to the normalization and background subtraction. Applying the AGS concept the covariance matrix  $V$  of the experimental transmission can be calculated by:

$$V = U_u + S(\eta)S(\eta)^T, \quad (4.1)$$

where  $U_u$  is a diagonal matrix containing the contribution of all uncorrelated uncertainty components. The matrix  $S$  contains the contribution of the components  $\eta = \{N, K_{in}, K_{out}\}$  creating correlated components. The uncertainty due to the dead time correction can be neglected. The experimental details, which are required to perform a resonance analysis on the data, are summarized in the Appendix.

## Acknowledgements

This work was supported by the EUFRAT open access programme of the Joint Research Centre.

## References

- [1] P. Schillebeeckx, B. Becker, Y. Danon, K. Guber, H. Harada, J. Heyse, A.R. Junghans, S. Kopecky, C. Massimi, M.C. Moxon, N. Otuka, I. Sirakov and K. Volev, "Determination of resonance parameters and their covariances from neutron induced reaction cross section data", Nucl. Data Sheets 113 (2012) 3054 – 3100.
- [2] A. Bensussan and J.M. Salomé, "GELINA: A modern accelerator for high resolution neutron time of flight experiments", Nucl. Instr. Meth. 155 (1978) 11 – 23.
- [3] W. Mondelaers and P. Schillebeeckx, "GELINA, a neutron time-of-flight facility for neutron data measurements", Notiziario Neutroni e Luce di Sincrotrone 11 (2006) 19 – 25.
- [4] D. Tronc, J.M. Salomé and K.H. Böckhoff, "A new pulse compression system for intense relativistic electron beams", Nucl. Instr. Meth. 228 (1985) 217 – 227.
- [5] J.M. Salomé and R. Cools, "Neutron producing targets at GELINA", Nucl. Instr. Meth. 179 (1981) 13 – 19.
- [6] M.C. Moxon and J.B. Brisland, Technical Report AEA-INTEC-0630, AEA Technology (1991).
- [7] F. Gunsing, P. Schillebeeckx and V. Semkova, Summary Report of the Consultants' Meeting on EXFOR Data in Resonance Region and Spectrometer Response Function, IAEA Headquarters, Vienna, Austria, 8-10 October 2013, INDC(NDS)-0647 (2013), [https://www-nds.iaea.org/index-meeting-crp/CM-RF-2013/\(03/05/2016\)](https://www-nds.iaea.org/index-meeting-crp/CM-RF-2013/(03/05/2016)).
- [8] C. Paradela et al. "Neutron resonance analysis for nuclear safeguards and security applications", EPJ Web of Conferences. Vol. 146. EDP Sciences, 2017.

- [9] S. de Jonge, "Fast Time Digitizer Type 8514 A", Internal Report GE/DE/R/24/87, IRMM, Geel.
- [10] J. Gonzalez, C. Bastian, S. de Jonge, and K. Hofmans, "Modular Multi-Parameter Multiplexer MPPM. Hardware description and user guide", Internal Report GE/R/INF/06/97, IRMM, Geel.
- [11] <https://www.mitutoyo.co.jp/eng/> (03/06/2016).
- [12] B. Becker, C. Bastian, J. Heyse, S. Kopecky and P. Schillebeeckx, "AGS – Analysis of Geel Spectra User's Manual", NEA/DB/DOC(2014)4.
- [13] B. Becker, C. Bastian, F. Emiliani, F. Gunsing, J. Heyse, K. Kauwenberghs, S. Kopecky, C. Lampoudis, C. Massimi, N. Otuka, P. Schillebeeckx and I. Sirakov, "Data reduction and uncertainty propagation of time-of-flight spectra with AGS", J. of Instrumentation, 7 (2012) P11002 – 19.
- [14] N. Otuka, E. Dupont, *et al.*, "Towards a More Complete and Accurate Experimental Nuclear Reaction Data Library (EXFOR): International Collaboration Between Nuclear Reaction Data Centres (NRDC)", Nucl. Data Sheets 120 (2014) 272-276.
- [15] N. Otuka, A. Borella, S. Kopecky, C. Lampoudis, and P. Schillebeeckx, "Database for time-of-flight spectra with their covariances", J. Korean Phys. Soc. 59 (2011) 1314 – 1317.
- [16] I. Sirakov, B. Becker, R. Capote, E. Dupont, S. Kopecky, C. Massimi, and P. Schillebeeckx, "Results of total cross section measurements for  $^{197}\text{Au}$  in the neutron energy region from 4 to 108 keV at GELINA", Eur. Phys. J. A 49 (144) (2013) 1.

# Appendix

## A. SUMMARY OF EXPERIMENTAL DETAILS

### A. 1 Experiment description (ID 1)

<b>1. Main Reference</b>		[a]
<b>2. Facility</b>	GELINA	[b]
<b>3. Neutron production</b> Neutron production beam Nominal average beam energy Nominal average current Repetition rate (pulses per second) Pulse width Primary neutron production target Target nominal neutron production intensity	Electron 100 MeV 50 $\mu$ A 800 Hz 2 ns Mercury cooled depleted uranium 3.4 x10 <sup>13</sup> s <sup>-1</sup>	
<b>4. Moderator</b> Primary neutron source position in moderator Moderator material Moderator dimensions (internal) Density (moderator material) Temperature (K) Moderator-room decoupler (Cd, B, ...)	Above and below uranium target 2 water filled Be-containers around U-target 2 x (14.6 cm x 21 cm x 3.9 cm) 1 g/cm <sup>3</sup> Room temperature None	
<b>5. Other experimental details</b> Measurement type Method (total energy, total absorption, ...) Flight Path length (m) (moderator centre-detector front face) Flight path direction Neutron beam dimensions at sample position Neutron beam profile Overlap suppression Other fixed beam filters	Transmission Good transmission geometry L = 10.860 (1) m 18° with respect to normal of the moderator face viewing the flight path 10 mm in diameter - 4 mm Cd overlap filter Na, Co, Ag, W, Pb	[c][d]
<b>6. Detector</b> Type Material Surface Dimensions Thickness (cm) Detector(s) position relative to neutron beam Detector(s) solid angle	Scintillator Li-glass 76 mm x 76 mm square 6.35 mm In the beam -	
<b>Sample</b> <b>7.</b> Type (metal, powder, liquid, crystal) Chemical composition Sample composition (at/b) Temperature Sample mass (g) Geometrical shape (cylinder, sphere, ...)	Metal <sup>103</sup> Rh (100 at %) 5.4987 (2) x 10 <sup>-4</sup> at/b 20 °C 0.58894 (2) g Square plate	

Surface dimension	626.20 (2) mm <sup>2</sup>	
Nominal thickness (mm)	0.075 mm	
Containment description	None	
<b>Data Reduction Procedure</b>		[d][e]
8. Dead time correction	Done (< factor 1.2)	
Back ground subtraction	Black resonance technique	
Flux determination (reference reaction, ...)	-	
Normalization	1.0000 (25)	
Detector efficiency	-	
Self-shielding	-	
Time-of-flight binning	Zone length      bin width	
	10240      2 ns	
	4096      4 ns	
	4096      8 ns	
	4096      16 ns	
	4096      32 ns	
	4096      64 ns	
	6144      128 ns	
	28672      64 ns	
<b>Response function</b>		
9. Initial pulse	Normal distribution, FWHM = 2 ns	
Target / moderator assembly	Numerical distribution from MC simulations	[f][g]
Detector	Analytical function defined in REFIT manual	[h]

## A. 2 Experiment description (ID 2)

<b>1. Main Reference</b>		[a]
<b>2. Facility</b>	GELINA	[b]
<b>3. Neutron production</b>		
Neutron production beam	Electron	
Nominal average beam energy	100 MeV	
Nominal average current	50 $\mu$ A	
Repetition rate (pulses per second)	800 Hz	
Pulse width	2 ns	
Primary neutron production target	Mercury cooled depleted uranium	
Target nominal neutron production intensity	$3.4 \times 10^{13} \text{ s}^{-1}$	
<b>4. Moderator</b>		
Primary neutron source position in moderator	Above and below uranium target	
Moderator material	2 water filled Be-containers around U-target	
Moderator dimensions (internal)	2 x (14.6 cm x 21 cm x 3.9 cm)	
Density (moderator material)	1 g/cm <sup>3</sup>	
Temperature (K)	Room temperature	
Moderator-room decoupler (Cd, B, ...)	None	
<b>5. Other experimental details</b>		
Measurement type	Transmission	

Method (total energy, total absorption, ...)	Good transmission geometry	[c][d]
Flight Path length (m) (moderator centre-detector front face)	L = 10.860 (1) m	
Flight path direction	18° with respect to normal of the moderator face viewing the flight path	
Neutron beam dimensions at sample position	10 mm in diameter	
Neutron beam profile	-	
Overlap suppression	4 mm Cd overlap filter	
Other fixed beam filters	Na, Co, Ag, W, Pb	
<b>6. Detector</b>		
Type	Scintillator	
Material	Li-glass	
Surface Dimensions	76 mm x 76 mm square	
Thickness (cm)	6.35 mm	
Detector(s) position relative to neutron beam	In the beam	
Detector(s) solid angle	-	
<b>7. Sample</b>		
Type (metal, powder, liquid, crystal)	Metal	
Chemical composition	<sup>103</sup> Rh (100 at %)	
Sample composition (at/b)	1.0818 (3) x 10 <sup>-3</sup> at/b	
Temperature	20 °C	
Sample mass (g)	4.63518 (3) g	
Geometrical shape (cylinder, sphere, ...)	Square plate	
Surface dimension	2505.3 (8) mm <sup>2</sup>	
Nominal thickness (mm)	0.15 mm	
Containment description	None	
<b>8. Data Reduction Procedure</b>		[d][e]
Dead time correction	Done (< factor 1.2)	
Back ground subtraction	Black resonance technique	
Flux determination (reference reaction, ...)	-	
Normalization	1.0000 ± 0.0025	
Detector efficiency	-	
Self-shielding	-	
Time-of-flight binning	<div>Zone length      bin width</div> <div>10240          2 ns</div> <div>4096          4 ns</div> <div>4096          8 ns</div> <div>4096          16 ns</div> <div>4096          32 ns</div> <div>4096          64 ns</div> <div>6144          128 ns</div> <div>28672          64 ns</div>	
<b>9. Response function</b>		
Initial pulse	Normal distribution, FWHM = 2 ns	[f][g]
Target / moderator assembly	Numerical distribution from MC simulations	
Detector	Analytical function defined in REFIT manual	[h]



**A. 3 Experiment description (ID 3)**

<b>1. Main Reference</b>		[a]
<b>2. Facility</b>	GELINA	[b]
<b>3. Neutron production</b> Neutron production beam Nominal average beam energy Nominal average current Repetition rate (pulses per second) Pulse width Primary neutron production target Target nominal neutron production intensity	Electron 100 MeV 3 $\mu$ A 50 Hz 2 ns Mercury cooled depleted uranium 3.4 x10 <sup>13</sup> s <sup>-1</sup>	
<b>4. Moderator</b> Primary neutron source position in moderator Moderator material  Moderator dimensions (internal) Density (moderator material) Temperature (K) Moderator-room decoupler (Cd, B, ...)	Above and below uranium target  2 water filled Be-containers around U-target 2 x (14.6 cm x 21 cm x 3.9 cm) 1 g/cm <sup>3</sup> Room temperature None	
<b>5. Other experimental details</b> Measurement type Method (total energy, total absorption, ...) Flight Path length (m) (moderator centre-detector front face) Flight path direction  Neutron beam dimensions at sample position Neutron beam profile Overlap suppression Other fixed beam filters	Transmission Good transmission geometry L = 10.860 (1) m  18° with respect to normal of the moderator face viewing the flight path 10 mm in diameter  - None Na, Co, Ag, W, Pb	[c][d]
<b>6. Detector</b> Type Material Surface Dimensions Thickness (cm) Detector(s) position relative to neutron beam Detector(s) solid angle	Scintillator Li-glass 76 mm x 76 mm square 6.35 mm In the beam -	
<b>7. Sample</b> Type (metal, powder, liquid, crystal) Chemical composition Sample composition (at/b)  Temperature Sample mass (g)  Geometrical shape (cylinder, sphere, ...) Surface dimension	Metal <sup>103</sup> Rh (100 at %) (1) 2.1295 (4) x 10 <sup>-3</sup> at/b (2) 2.16771 (5) x 10 <sup>-3</sup> at/b (3) 1.07940 (6) x 10 <sup>-3</sup> at/b 20 °C (1) 8.98856 (6) g (2) 9.24940 (7) g (3) 4.56431 (3) g Square plate (1) 2467.8 (5) mm <sup>2</sup> (2) 2494.69 (6) mm <sup>2</sup>	

Nominal thickness (mm)	(3) 2472.28 (14) mm <sup>2</sup>	
Containment description	0.75 mm	
	None	
<b>8. Data Reduction Procedure</b>		[d][e]
Dead time correction	Done (< factor 1.2)	
Back ground subtraction	Black resonance technique	
Flux determination (reference reaction, ...)	-	
Normalization	1.0000 ± 0.0025	
Detector efficiency	-	
Self-shielding	-	
Time-of-flight binning	Zone length      bin width	
	16384      1 ns	
	10240      2 ns	
	8192      4 ns	
	8192      8 ns	
	6144      16 ns	
	6144      32 ns	
	4096      64 ns	
	4096      512 ns	
	1024      4096 ns	
	1024      16384 ns	
<b>9. Response function</b>		
Initial pulse	Normal distribution, FWHM = 2 ns	
Target / moderator assembly	Numerical distribution from MC simulations	[f][g]
Detector	Analytical function defined in REFIT manual	[h]

## B. Data format

Column	Content	Unit	Comment
1	Energy	eV	Relativistic relation using a fixed flight path length (L = 10.860 m)
2	t <sub>i</sub>	ns	
3	t <sub>h</sub>	ns	
4	Y <sub>exp</sub>		Transmission
5	Total Uncertainty		
6	Uncorrelated uncertainty		Uncorrelated uncertainty due to counting statistics
7	AGS-vector (K)		Background model uncertainty (u <sub>K</sub> /K=3 %)
8	AGS-vector (N)		Normalization (u <sub>N</sub> /N = 0.25 %)

Comments from the authors:

- The AGS concept was used to derive the experimental transmission

$$T_{exp} = N \frac{C_{in} - KB_{in}}{C_{out} - KB_{out}},$$

and to propagate the uncertainties, both the uncorrelated due to counting statistics and the uncertainty due to the normalization and the background contributions.

- The quoted uncertainties are standard uncertainties at 1 standard deviation

### B.1 DATA (ID 1)

E/ eV	$t_l$ / ns	$t_h$ / ns	$Y_{exp}$	$u_t$	$u_u$	AGS K	N
0.49993	1110400	1110528	0.9331	0.0294	0.0293	-0.000281	0.00233
0.50004	1110272	1110400	0.9454	0.0298	0.0297	-0.000212	0.00236
...	...	...	...	...	...	...	...
0.99986	785152	785280	0.76910	0.00666	0.00638	-0.000102	0.00192
1.00018	785024	785152	0.76990	0.00668	0.00639	-0.000102	0.00192
...	...	...	...	...	...	...	...
4.9990	351104	351168	1.0287	0.0357	0.0356	0.000337	0.00256
5.0018	351040	351104	0.9948	0.0350	0.0349	0.000074	0.00248

### B.2 DATA (ID 2)

E/ eV	$t_l$ / ns	$t_h$ / ns	$Y_{exp}$	$u_t$	$u_u$	AGS K	N
0.49990	1110400	1110528	0.9235	0.0306	0.0305	-0.000132	0.00230
0.50018	1110272	1110400	0.8987	0.0299	0.0298	-0.000276	0.00224
...	...	...	...	...	...	...	...
0.99986	785152	785280	0.5964	0.0057	0.00550	-0.000178	0.00148
1.00018	785024	785152	0.5914	0.0056	0.00548	-0.000180	0.00147
...	...	...	...	...	...	...	...
4.9990	351104	351168	0.9957	0.0356	0.0355	0.000013	0.00248
5.0018	351040	351104	1.0350	0.0386	0.0385	0.000337	0.00257

### B.3 DATA (ID 3)

E/ eV	$t_l$ / ns	$t_h$ / ns	$Y_{exp}$	$u_t$	$u_u$	AGS K	N
0.009996	7852032	7854080	0.29622	0.01576	0.01574	-0.00031	0.00073
0.010001	7849984	7852032	0.28892	0.01565	0.01563	-0.00032	0.00072
...	...	...	...	...	...	...	...
1.99994	555136	555264	0.74695	0.02113	0.02104	-0.00019	0.00188
2.00086	555008	555136	0.74216	0.02122	0.02114	-0.00019	0.00184
...	...	...	...	...	...	...	...
4.9999	351104	351168	0.90660	0.16564	0.16542	-0.00167	0.00224
5.0018	351040	351104	0.96061	0.17892	0.17890	-0.00075	0.00238

## References

- [a] Y. K. Kim, V. Chavan, C. Paradela, S. I. Bak, G. Alaerts, J. Heyse, S. Kopecky, A. Oprea, P. Schillebeeckx, R. Wynants and S. W. Hong, " Results of time-of-flight transmission measurements for  $^{103}\text{Rh}$  at a 10 m station of GELINA ", INDC(EUR) 0033, 2019.
- [b] W. Mondelaers and P. Schillebeeckx, "GELINA, a neutron time-of-flight facility for neutron data measurements", *Notiziario Neutroni e Luce di Sincrotrone*, 11 (2006) 19 – 25.
- [c] B. Becker, C. Bastian, F. Emiliani, F. Gunsing, J. Heyse, K. Kauwenberghs, S. Kopecky, C. Lampoudis, C. Massimi, N. Otuka, P. Schillebeeckx and I. Sirakov, "Data reduction and uncertainty propagation of time-of-flight spectra with AGS", *J. of Instrumentation*, 7 (2012) P11002 – 19.
- [d] P. Schillebeeckx, B. Becker, Y. Danon, K. Guber, H. Harada, J. Heyse, A.R. Junghans, S. Kopecky, C. Massimi, M.C. Moxon, N. Otuka, I. Sirakov and K. Volev, "Determination of resonance parameters and their covariances from neutron induced reaction cross section data", *Nuclear Data Sheets* 113 (2012) 3054 – 3100.
- [e] B. Becker, C. Bastian, F. Emiliani, F. Gunsing, J. Heyse, K. Kauwenberghs, S. Kopecky, C. Lampoudis, C. Massimi, N. Otuka, P. Schillebeeckx and I. Sirakov, "Data reduction and uncertainty propagation of time-of-flight spectra with AGS", *J. of Instrumentation*, 7 (2012) P11002 – 19.
- [f] M. Flaska, A. Borella, D. Lathouwers, L.C. Mihailescu, W. Mondelaers, A.J.M. Plompen, H. van Dam, T.H.J.J. van der Hagen, "Modeling of the GELINA neutron target using coupled electron–photon–neutron transport with the MCNP4C3 code", *Nucl. Instr. Meth. A* 531 (2004) 392–406.
- [g] D. Ene, C. Borcea, S. Kopecky, W. Mondelaers, A. Negret and A.J.M. Plompen, "Global characterisation of the GELINA facility for high-resolution neutron time-of-flight measurements by Monte Carlo simulations", *Nucl. Instr. Meth. A* 618 (2010) 54 - 68.
- [h] M.C. Moxon and J.B. Brisland, Technical Report AEA-INTEC-0630, AEA Technology (1991).



---

Nuclear Data Section  
International Atomic Energy Agency  
P.O. Box 100  
A-1400 Vienna  
Austria

---

e-mail: [nds.contact-point@iaea.org](mailto:nds.contact-point@iaea.org)  
fax: (43-1) 26007  
telephone: (43-1) 2600 21725  
Web: <http://www-nds.iaea.org/>